Half-Quadratic Cost Functions for Phase Unwrapping

Mariano Rivera and Jose L. Marroquin

Centro de Investigacion en Matematicas A.C.,

Apdo. Postal 402, Guanajuato, Gto. Mexico 36000

We present a generic regularized formulation, based on robust half–quadratic regularization, for unwrapping noisy and discontinuous wrapped phase maps. Two cases are presented: the convex and the non–convex one. The unwrapped phase with the convex formulation is unique and robust to noise; however, the convex function solution is deteriorated by real discontinuities in phase maps; therefore, we also present a non–convex formulation which, with a parameter continuation strategy, shows a superior performance.

OCIS codes: 100.2650, 100.5070, 120.5050, 100.3020, 100.3190.

As the result of many optical experiments, one obtains a wrapped phase map which may be modelled as $g_r = W(\phi_r + \eta_r)$, where $r = (x, y)$ represents a site in a regular lattice L, η is additive noise and W is the (non-linear) wrapping operator: $W(x) = x + 2k\pi$, with k integer such that $W(x) \in [-\pi, \pi)$. Then, the phase unwrapping process consists on recovering a phase field ϕ with given characteristics (i.e., a smooth or piecewise smooth field) from the wrapped phase, g, that presents spurious phase jumps due to the wrapping operator.

From the wrapped phase map, it is possible to compute the phase differences $\Delta g_{rs} \stackrel{def}{=} g_r - g_s$ between contiguous (vertical or horizontal) pixels; these phase differences are in the interval $[-2\pi, 2\pi)$. When the real phase differences $\Delta \hat{f}_{rs} = \Delta\phi_{rs} + \Delta\eta_{rs}$ are confined to the interval $[-\pi, \pi)$, the equation:

$$\Delta \hat{f}_{rs} - W(\Delta g_{rs}) = 0, \tag{1}$$

is satisfied for all the neighboring pixel pairs and the unwrapping process is achieved by a simple two-dimensional integration of the wrapped difference field, $W(\Delta g_{rs})$. However, phase discontinuities in $\hat{f}$ greater than π generate inconsistencies in the field $W(\Delta g_{rs})$, so that path dependent algorithms fail. Inconsistencies are located at those sites where $\Delta \times W(\Delta g_{rs}) \neq 0$, with $\Delta\times$ as the discrete version of the rotational operator. The unwrapping of inconsistent phase maps is ill-posed because information provided by the data and the model (1) is (in general) not sufficient for an accurate estimation of the phase $\hat{f}$. In the framework of Bayesian regularization,[1] the regularized solution, f, (estimate of the true phase $\hat{f}$) is computed by minimizing a cost function $U(f) = D(f) + \lambda R(f)$. The data term D establishes that the reconstruction, f, should be consistent with the data, g and is chosen as the negative log-likelihood [see model (1)]: $D(f) = \sum_{\langle r,s \rangle} [f_r - f_s - W(\Delta g_{rs})]^2$. The regularization term, R, imposes a penalty for violating the *a priori* assumptions. The relative contribution of each term to the global cost is weighted by the positive parameter λ. The prior constraints are, in this framework, incorporated in the form of a Markov Random Field model for f, so that $R(f)$ takes the form of a sum over the cliques $\langle r, s \rangle$, of a neighborhood system, of a set of "potential functions" supported on those cliques: $R(f) = \sum_{\langle r,s \rangle} \rho(f; r, s)$. One

may use, for example, the neighborhood system: $N_r = \{s \in L : 0 < |r - s| \leq \sqrt{2}\}$, so that $\langle r, s\rangle$ corresponds to horizontal, vertical and diagonal first neighbor pixel pairs: $\langle r, s\rangle = \{(r, s) : r \in L, s \in N_r\}$. Choosing ρ as a quadratic function[1] one obtains:

$$U(f) = \sum_{\langle r,s\rangle} \left[\alpha_{rs}^2 + \lambda\beta_{rs}^2\right], \tag{2}$$

where $\alpha_{rs} \stackrel{def}{=} f_r - f_s - W(\Delta g_{rs})$ and $\beta_{rs} \stackrel{def}{=} f_r - f_s$. Note that for $\lambda = 0$ one obtains the usual least squares formulation. The phase unwrapped with (2) has the problem of producing a reduced dynamic range and an over–smoothing of the real phase discontinuities because the term β_{rs}^2 penalizes large gradient magnitudes in the unwrapped phase, f. Additionally, the quadratic term α_{rs}^2 is based on the wrong assumption of residuals [see model (1)] with a Gaussian distribution.

To address these problems, and also problems associated with phase steps larger than π in the true phase, we propose to find the unwrapped phase as the minimizer of:

$$U_{hq}(f, l) = \sum_{\langle r,s\rangle} \rho_{hq}(f, l; r, s) = \sum_{\langle r,s\rangle} \left\{l_{rs}^2(\alpha_{rs}^2 + \lambda\beta_{rs}^2) + \Psi(l_{rs})\right\}, \tag{3}$$

where α_{rs} and β_{rs} are defined above, $l_{rs}^2 \in [0, 1]$ is a continuous auxiliary variable that acts as an outlier detector and Ψ is a convex potential function. The potential ρ_{hq} in (3) is HQ in the sense that: it is quadratic with respect to f when l is fixed and convex with respect to l when f is fixed.[2,3,4,5] The behavior of the potential ρ_{hq} may be understood by considering that $l_{rs}^2 \approx 0$ if there is a discontinuity (an edge) or an inconsistency between the sites r and s, and $l_{rs}^2 \approx 1$ otherwise. Thus, the first term in (3) constrains the phase differences of the unwrapped phase to be close to the observed phase differences unless the corresponding l variable is close to one.

The potential Ψ controls the threshold for detecting an edge. If $\Psi(l_{rs})$ is too small everywhere, one may have an edge over–detection; on other hand, if it is too large, ones does not detect any edge, and as a consequence the solution is homogeneously smoothed [i.e. (3) behaves as (2)].

Cost functions of the form (3) can be minimized by performing an alternated minimization of U_{hq} with respect to the variables f and l.[2,3] This is expressed in the following algorithm:

Alternated Minimization Algorithm (AM): *Set $t = 0$ and $l_{rs} = 1\ \forall\langle r, s\rangle$, then iterate until convergence:*

1. *Solve for f the linear system, keeping l fixed, that results from: $\nabla_f U_{hq}(f, l) = 0$. This is*

$$\sum_{s \in N_r} 2l_{rs}^2 \left(\alpha_{rs} \frac{\partial \alpha_{rs}}{\partial f_r} + \lambda \beta_{rs} \frac{\partial \beta_{rs}}{\partial f_r} \right) = 0 \tag{4}$$

   for all $r \in L$.

2. *Update l, keeping f fixed, by solving the system that result from: $\nabla_l U_{hq}(f, l) = 0$. The keypoint, in half–quadratic potentials, is to choose a potential Ψ such that this step leads one to a closed form solution, i.e. $l_{rs}^2 = w\left(\alpha_{rs}^2 + \lambda \beta_{rs}^2\right)$.*

The second step in the AM algorithm depends on the specific potential Ψ. We distinguish two cases:

Convex case. The main advantage of the minimization of convex functions is that one always computes the global minimum independently of the initial guess. Note that if one makes $\lambda = 0$ and defines the function $\hat{\rho}$ as:

$$\hat{\rho}(\alpha_{rs}) \stackrel{def}{=} \int_0^{\alpha_{rs}} 2w(x^2)x dx. \tag{5}$$

Then, the minimum f^* of U_{hq} computed using the AM algorithm will also be a minimum of

$$\hat{U}_{hq}(f,l) = \sum_{\langle r,s \rangle} \hat{\rho}\left(\alpha_{rs}\right). \tag{6}$$

Since

$$\frac{\partial \hat{U}_{hq}}{\partial f_r} = \sum_{s \in N_r} \hat{\rho}^{'}(\alpha_{rs}) \frac{\partial \alpha_{rs}}{\partial f_r} = \sum_{s \in N_r} 2w(\alpha_{rs}^2)\alpha_{rs} \frac{\partial \alpha_{rs}}{\partial f_r}.$$

So that (3) holds at the critical points of (6) when $l_{rs}^2 = w(\alpha_{rs}^2)$ (i.e. for the optimal l_{rs}). This means that if one chooses Ψ (and hence w) such that $\hat{\rho}$ is convex, function (6) [and hence (3)] will have an unique global minimum and the AM algorithm will converge to it. In particular one can choose Ψ such that potential $\hat{\rho}$ corresponds to the convex Huber potential:[2,4] $\hat{\rho}(\alpha_{rs}) = \alpha_{rs}^2$ if $|\alpha_{rs}| \leq \varepsilon$, $\hat{\rho}(\alpha_{rs}) = 2\varepsilon|\alpha_{rs}| - \varepsilon^2$, otherwise. Note that in this case there is no need to define Ψ explicitly. The minimization w.r.t. l results in the closed–form solution :

$$l_{rs}^2 = w(\alpha_{rs}^2) = \frac{\hat{\rho}^{'}(\alpha_{rs})}{2\alpha_{rs}} = \begin{cases} 1 & \sqrt{\alpha_{rs}^2} \leq \varepsilon \\ \varepsilon / \sqrt{\alpha_{rs}^2} & \text{otherwise,} \end{cases} \tag{7}$$

where ε is a small positive constant (we use in our experiments $\varepsilon = 0.1$).

Non–convex case. In this case, we use $\lambda \neq 0$, and $\Psi(l_{rs}) = \mu(l_{rs} - 1)^2$, where μ is a positive parameter that controls an over–detection of outliers. Thus, we obtain:

$$l_{rs}^2 = w(\alpha_{rs}^2 + \lambda\beta_{rs}^2) = \frac{\mu}{[\mu + (\alpha_{rs}^2 + \lambda\beta_{rs}^2)]^2}. \tag{8}$$

That corresponds to the commonly used non-convex Geman–McClure potential,[2,3,4] $\hat{\rho}(\sqrt{\alpha_{rs}^2 + \lambda\beta_{rs}^2}) = (\alpha_{rs}^2 + \lambda\beta_{rs}^2)/(\mu + \alpha_{rs}^2 + \lambda\beta_{rs}^2)$. Note that in this case the edge detection process, l, is driven by the inconsistencies and the phase gradient magnitude. We implement a parameter continuation strategy in order to lead the algorithm to a

"good" local minimum and to eliminate the dynamic range reduction on f, because of the penalization of the gradient magnitude. The parameter continuation is implemented by setting $\lambda^2 \equiv \lambda(t) = \lambda_0 \times 0.5^{c_1 t}$ and $\mu \equiv \mu(t) = \mu_0 \times 0.5^{c_2 t}$, where c_1 and c_2 are positive parameters and t is the number of iteration. Therefore, the edge sensibility and the gradient contribution is reduced every iteration. In our experiments, we set: $c_1 = c_2 = 1/20$ and the initial values of the parameters: $\lambda_0 = 10$ and $\mu_0 = 1$. Now we present and discuss some numerical experiments that illustrate the performance of the convex and non-convex HQ phase unwrapping techniques. Figure 1 shows the test phases. Panel 1–(a) shows a synthetic wrapped phase previously corrupted with uniform noise with amplitude equal to 3.0 radians. The wrapped phases in panels 1–(b) and 1–(c) correspond to real EPSI images: the wrapped phase in panel 1–(b) shows the relative deformation of a steel plate when a thermal stress is applied. The wrapped phase in panel 1–(c) shows the relative deformation of a steel plate with a fracture when a mechanical stress is applied.

Figure 2 shows the unwrapped phase, of the wrapped phase in 1–(a), with different methods. First column corresponds to the unwrapped phase, middle column to the rewrapped phase and last column to the edge field, l^2. With the exception of the case illustrated in row 2–(d), we use 8 neighbors in all the cases, which improves significantly the quality of the unwrapped phase [compare 2–(d) with 2–(e)]. In this experiment, one notes the bad performance of the convex potential [row 2–(c)]. However, the convex function can be adequate for low noise levels which show that, with the advantage of the solution being unique [these two cases are compared in figure 3]. The algorithm based on non–convex functions and the parameter continuation

strategy produced in all the cases (synthetic and real test wrapped phases) the best results [see rows 3–(c) and 3–(d)]. The phase discontinuity in the wrapped phase in panel 1–(c) is better preserved in the unwrapped phase shown in row 3–(d). The drawback, in the non-convex case, is the additional parameters that need be tuned and the computational cost that results in a slow parameter continuation. The computational times (and the number of iterations) for the wrapped phases shown in Fig. 3, were: a) 57 secs. (31 iter.), b) 177 secs. (75 iter.), c) 385 secs. (223 iter.) and d) 618 secs. (320 iter.). Each iteration corresponds to solving the linear system (4) with the conjugate gradient algorithm and updating the l field.

We observed a degradation of the non-convex unwrapping method for wrapped phase with a very low SNR; in such case, the algorithm is easy trapped by a local minima. For instance, if the wrapped phase in 1–(a) is corrupted with uniform noise with amplitude equal to 4.0 radians, then the unwrapped phase contains discontinuities as those observed in Fig. 2–(b). As in the case of Figs. 2–(b) and (c), the rewrapped phase in this case is indistinguishable from the original wrapped phase. An opportunity for future research is to improve the performance of the method for wrapping phases with low SNR.

The authors thank to R. Rodriguez-Vera for proving data used in the experiments. The authors were partially supported by CONACYT (Mexico) under grant 40722A1.

References

1. J.L. Marroquin and M. Rivera, J. Opt. Soc. Am. A, **12**, 2393 (1995).
2. M.J. Black and A. Rangarajan, Int. J. Comput. Vis., **19**, 57 (1996).
3. P. Charbonnier, L. Blanc-Féraud, G. Aubert and M. Barlaud, IEEE Trans. Image Process, **6**, 298 (1997).
4. M. Rivera, and J.L. Marroquin, Image and Vision Computing, **21**, 345 (2003).
5. M. Rivera and J.L. Marroquin, Comput. Vision Image Understand., **88**, 76 (2002).
6. D.C. Ghiglia and L.A. Romero, J. Opt. Soc. Am. A, **13**, 1999 (1996).

COMPLETE REFERENCES WITH TITLES

1. J.L. Marroquin and M. Rivera, "Quadratic regularization functional for phase unwrapping," J. Opt. Soc. Am. A, 12, 2393-2400 (1995).

2. M.J. Black and A. Rangarajan, "Unification of line process, outlier rejection, and robust statistics with application in early vision," Int. J. Comput. Vis., 19, 57–91 (1996).

3. P. Charbonnier, L. Blanc-Féraud, G. Aubert and M. Barlaud, "Deterministic edge-preserving regularization in computer imaging," IEEE Trans. Image Process, 6, 298–311 (1997).

4. M. Rivera, and J.L. Marroquin, "Efficient half-quadratic regularization with granularity control," Image and Vision Computing, 21, 345-357 (2003).

5. M. Rivera and J.L. Marroquin, "Adaptive rest condition potentials: Second order edge–preserving regularization," Comput. Vision Image Understand., 88, 76–93 (2002).

6. D.C. Ghiglia and L.A. Romero "Minimum Lp–norm two-dimensional phase unwrapping," J. Opt. Soc. Am. A, 13, 1999 (1996).

Figure Captions

Figure 1. Test wrapped phases: (a) synthetic, (b) deformation of a steel plate (ESPI), and (c) fracture in a steel plate (ESPI).

Figure 2. Each row shows, respectively, the unwrapped phase, rewrapping of the unwrapped phase and the l field with: (a) quadratic potential,[1] (b) the Ghiglia–Romero's L_0–Norm[6] [in our formulation it is equivalent to the Herbert–Leahy's non-convex HQ potential,[3] i.e. $\Psi(l_{rs}) = \mu(l_{rs}^2 - \ln(l_{rs}^2) - 1)$, where μ is the positive parameter that controls the outlier detection and with $\lambda = 0$], and the proposed HQ cost function with: (c) convex, (d) non-convex with 4 neighbors and (e) non-convex with 8 neighbors.

Figure 3. Results computed with the proposed method, in the same order as Fig. 2. Rows (a) and (b) with the convex HQ cost function, rows (c) and (d) with the non-convex one.

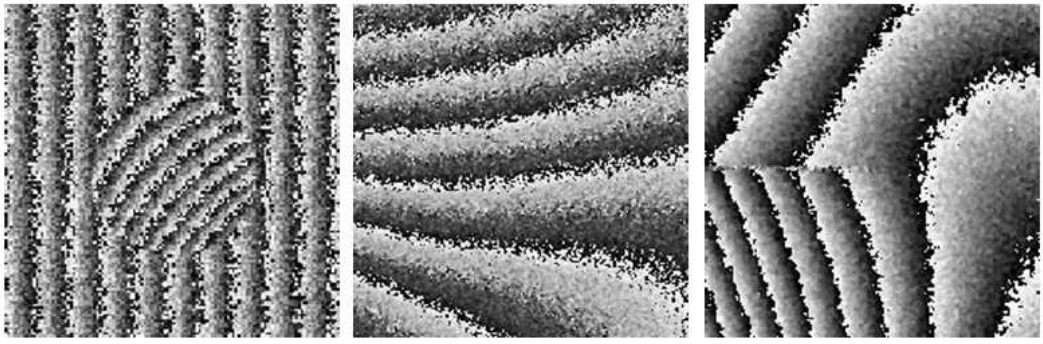

Fig. 1.

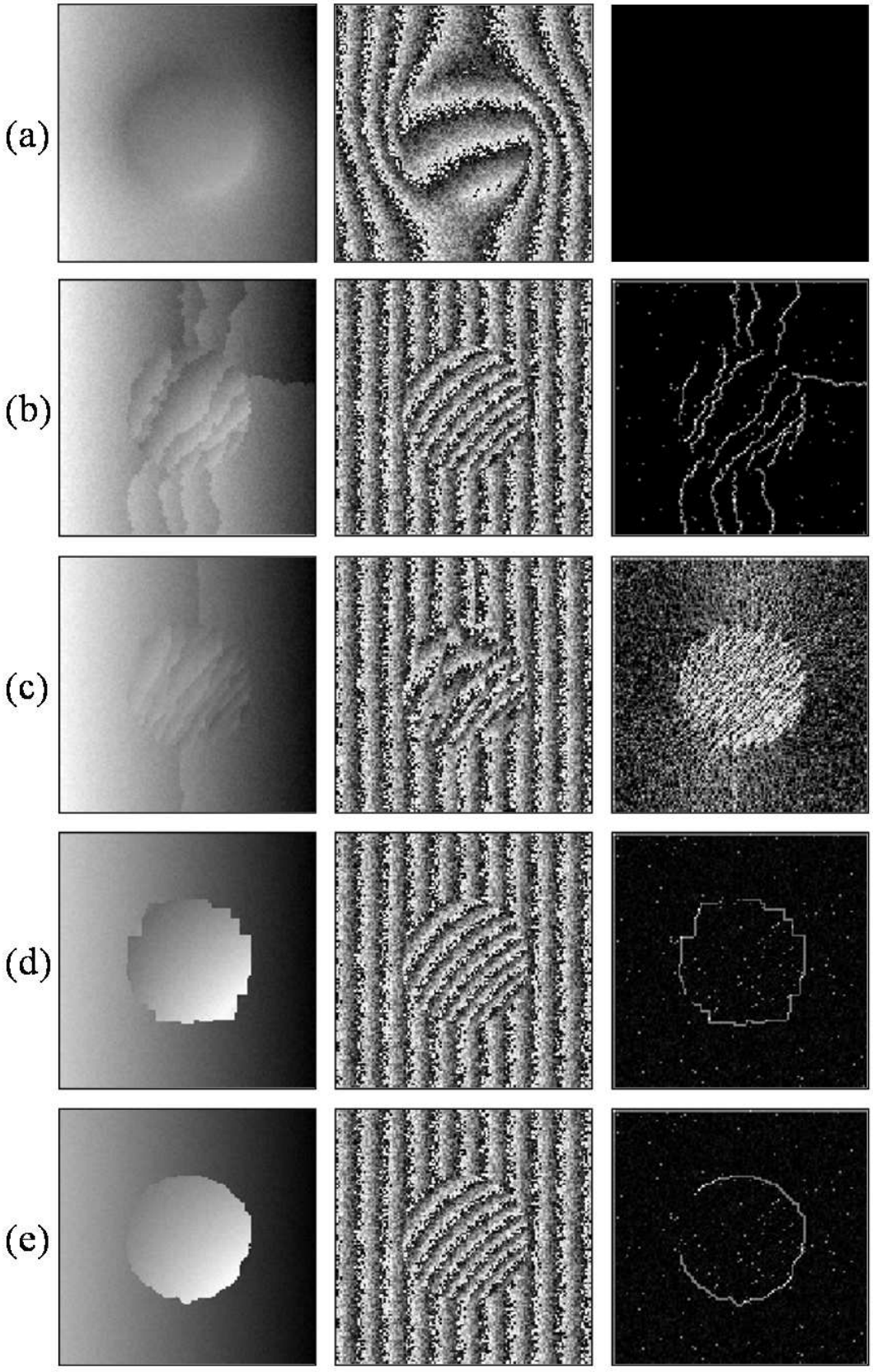

Fig. 2.

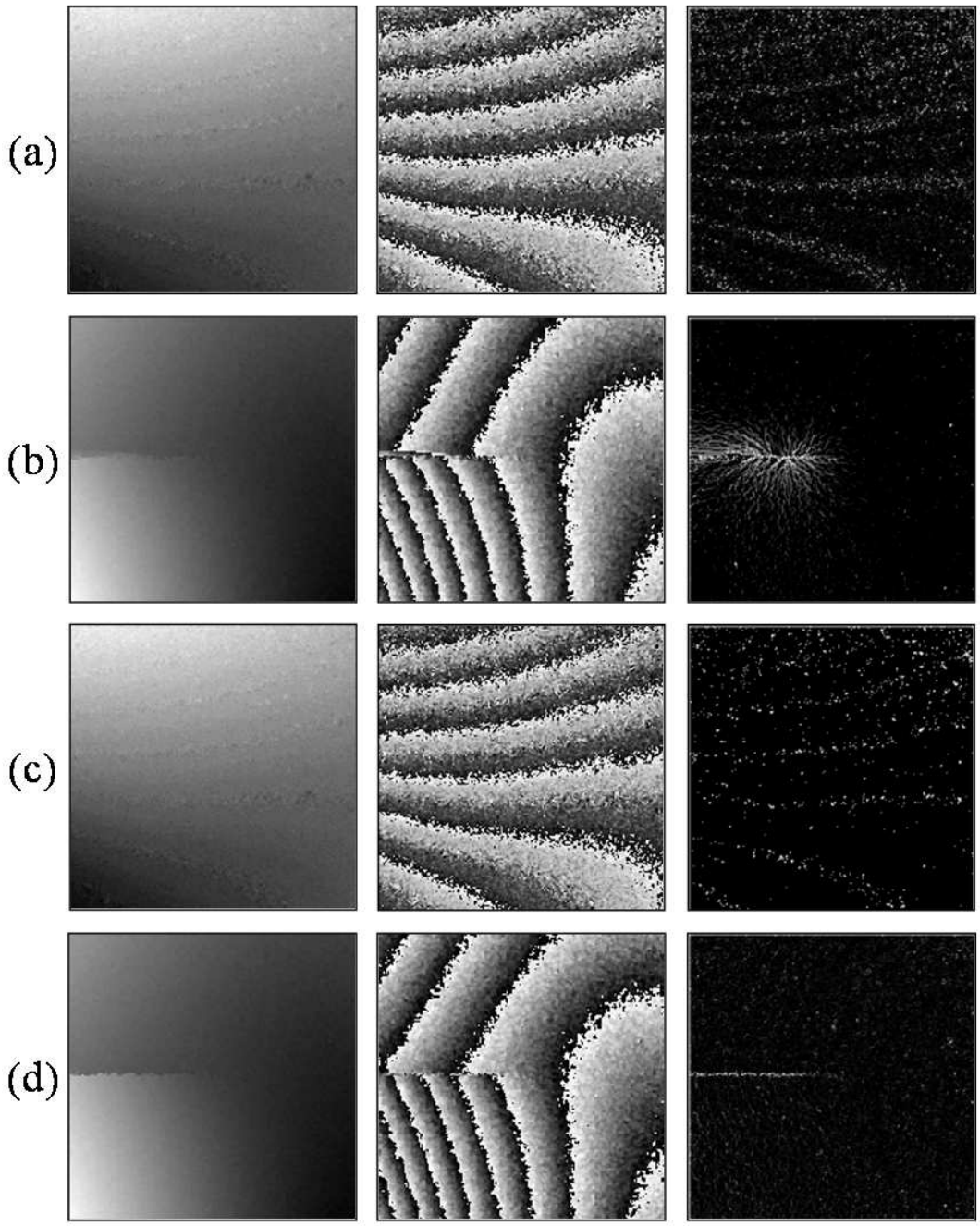

Fig. 3.